Premix Membrane Emulsification by Using a Packed Layer of Glass Beads

E. A. van der Zwan, C. G. P. H. Schroën, and R. M. Boom
Wageningen University – Food and Bioprocess Engineering Group, P.O. Box 8129, Wageningen 6700EV, The Netherlands

DOI 10.1002/aic.11508
Published online May 22, 2008 in Wiley InterScience (www.interscience.wiley.com).

Premix membrane emulsification is a very efficient process. Its prime disadvantage, depth fouling of the pores, could be avoided by using instead of a membrane, a packed layer of small particles, that can be resuspended and cleaned in suspension after emulsification. The effectiveness of emulsification with this system was measured. The energy density approach was extended to predict the droplet size as a function of pressure drop, bed height, and number of passes. Three different extensions to the model were compared, and a reasonable description was found for the resulting droplet size in all the experiments (167) for a four-parameter model. It is expected that the function derived can be helpful to describe conventional membrane homogenization, since a first comparison showed that the data obtained with the particle bed are similar to those obtained in literature with membranes. © 2008 American Institute of Chemical Engineers *AIChE J,* 54: 2190–2197, 2008

Introduction

Premix membrane emulsification is an emulsion production method which received much attention in past years. The method was introduced by Suzuki and coworkers.[1] A coarse premix emulsion, with large droplets and a wide droplet-size distribution, is pushed through a membrane with pores in the micrometer range. Here, the droplets are broken up into smaller droplets resulting in an emulsion with not only smaller droplets, but also a narrower droplet-size distribution at relatively low-energy costs, and relatively high-production rate.[1] Because of the narrow droplet-size distribution obtained, and the low-energy costs it has proven itself to be a good alternative for conventional emulsification methods, such as high-pressure homogenizers, colloid mills, and rotor-stator systems. Besides this, premix membrane emulsification is also a good alternative for other novel production methods, such as cross-flow membrane emulsification, and microchannel emulsification, because of its high-production rate. Its biggest disadvantage is its sensitivity to depth fouling of the membrane, depending on the components used in the formulation. For example, use of proteins as stabilizers will lead to heavy internal fouling and effective blockage in the pores.

Although many studies[2–6] have proven the effectiveness of the method, not much is known about the mechanisms of droplet breakup and coalescence in premix membrane emulsification. As a consequence, the effect of membrane geometry on droplet breakup is also not known. Besides this, it is common practice to pass the emulsion through the membrane several times to decrease the droplet size further.[2–6] From these studies it is clear that recirculation has a beneficial effect on both the droplet size and the droplet-size distribution. However, no quantitative description of these effects is available; it has not been tested, for example, whether the effect of two passes through a membrane is equivalent to one pass through a membrane with the same morphology, but twice the thickness.

A recent study[7] showed that premix membrane emulsification is dictated by three types of breakup:

- Snap-off due to localized shear forces.
- Breakup due to interfacial tension effects (Rayleigh and Laplace instabilities).
- Breakup due to steric hindrance between droplets.

Besides this, it could be shown qualitatively that there is a link between the geometry and the resulting droplet size. In

Correspondence concerning this article should be addressed to E. A. van der Zwan at this current address: 2190 Advanced Technology Center (ATC), Philips Consumer Lifestyle, Tussendiepen 4, 9206 AD Drachten, The Netherlands. E-mail: eduard.van.der.zwan@philips.com.

microfluidic devices with various layers of brick-like obstructions, the smallest droplets are found for an optimal number of layers. A low number of layers results in incomplete breakup, while a high-number of layers results in coalescence inside the structure, and, therefore, both situations away from the optimum result in bigger droplets.

In this work, a packed bed of small glass beads was used. The pore sizes and tortuosities are similar to those found in porous membranes. The morphology of the packed bed is very similar to the morphology of some membranes used for premix membrane emulsification (e.g., ceramic membranes made from a layer of packed, sintered particles), while the layer thickness can be varied more easily.

In addition, use of such a "dynamic membrane" for emulsification has the advantage that the system can be easily cleaned after emulsification: the particles are resuspended and then cleaned in suspension. In our case, rinsing with hot water was found to be sufficient. Subsequent renewed settling into a packed bed makes the system ready for use again. Such a setup could, therefore, be a practical alternative to using fixed membranes for systems with ingredients that would give depth fouling of the membrane pores.

In this article, we present a study on emulsification with glass bead beds, and compare this emulsification method briefly with premix membrane emulsification. To describe all the effects relevant to premix emulsification, such as the height of the bed, the number of recycles, or the transmembrane pressure, an energy density approach is used in which all mentioned factors are incorporated.

Theory

The starting point for the experiments, and the analysis thereof, is flow of a continuous phase through a bed of noncompressible particles. The pressure drop over the bed Δp_{bed} (Pa) is given by the Ergun relation[8]

$$\Delta p_{\text{bed}} = \frac{170\varepsilon^2 \eta_l v_{sl} H_{\text{bed}}}{(1-\varepsilon)^3 d_p^2} + \frac{1.75\varepsilon \rho_l v_{sl}^2 H_{\text{bed}}}{(1-\varepsilon)^3 d_p} \tag{1}$$

in which ε is the particle holdup [-], η_l is the dynamic viscosity of the liquid [$\text{Pa}\cdot\text{s}$], d_p is the particle diameter (m), ρ_l is the density of the liquid [$\text{kg}\cdot\text{m}^{-3}$], H_{bed} is the height of the particle bed (m), and v_{sl} is the superficial liquid speed [$\text{m}\cdot\text{s}^{-1}$]. The superficial liquid speed is calculated with

$$v_{sl} = \frac{J}{1-\varepsilon} \tag{2}$$

where J is the flux across the bed $\text{m}^3\cdot\text{s}^{-1}\cdot\text{m}^{-2} = \text{m}\cdot\text{s}^{-1}$, and the bed height is calculated with

$$H_{\text{bed}} = \frac{m_{\text{bed}}}{\rho_p \varepsilon A_{\text{col}}} \tag{3}$$

in which m_{bed} is the mass of the particle bed [1 – 8 g], ρ_p is the specific density of the particles [2518 $\text{kg}\cdot\text{m}^{-3}$], and A_{col} is the surface area of the column [$3.28\cdot10^{-4}$ m^2].

Although the Ergun relation is for one-phase flow only it can give a good estimation of the pressure drop for emulsions if the dispersed phase fraction is low (<10%; in this study we used 5%), and, thus, the density and dynamic viscosity of the liquid do not differ too much from the continuous phase.

In our system, not only the bed is present, but also a coarse support filter, which has to be taken into account. The pressure drop over the bed and the filter together, Δp [Pa] is

$$\Delta p = \Delta p_{\text{filter}} + \Delta p_{\text{bed}} \tag{4}$$

in which Δp_{filter} is the pressure drop across the filter, and Δp_{bed} is the pressure drop across the particle bed both in [Pa]. The pressure drop across the filter is estimated with the following equation (in parallel with the Ergun Eq. 1)

$$\Delta p_{\text{filter}} = \alpha_{\text{filter}} J^2 + \beta_{\text{filter}} J \tag{5}$$

in which J is the flux across the filter [$\text{m}^3\cdot\text{s}^{-1}\cdot\text{m}^{-2} = \text{m}\cdot\text{s}^{-1}$], α_{filter} is a fit parameter [$\text{kg}\cdot\text{m}^{-3}$], and β_{filter} is an other fit parameter [$\text{kg}\cdot\text{m}^{-2}\cdot\text{s}^{-1}$].

The flux across the particle bed is calculated from the mass flow Φ_m [$\text{kg}\cdot\text{s}^{-1}$], which we incorporated in the equation with

$$J = \frac{\Phi_m}{\rho_l A_{\text{col}}} \tag{6}$$

in which ρ_l is the density of the liquid, and A_{col} is the surface area of the column.

For continuous mechanical emulsification processes, Karbstein[9] derived a relation for the Sauter mean diameter of a homogenized emulsion $d_{3,2}$, and the specific energy density E_V

$$d_{3,2} = \alpha_{\text{drop}} E_V^{-\beta_{\text{drop}}} \tag{7}$$

in which α_{drop} [−] and β_{drop} [−], are constants that depend on the flow profile and on the homogenization method. Note that the Sauter mean diameter and the specific energy density have to be made dimensionless by division by an appropriate unit (see results and discussions section). In turbulent flow β_{drop} varies between 0.25 and 0.4, while in laminar flow it is 1. It should be noted that this is not a universal relation: use of a different formulation or different conditions can result in different values of the parameters.

In membrane emulsification methods, where the droplet diameter and the pore diameter are of the same order of magnitude, α_{drop} increases with increasing dispersed phase volume fraction, while β_{drop} has a value in between the values for turbulent and laminar flow.[10]

For the first pass through the membrane we can use the pressure drop Δp [Pa] instead of the specific energy density E_V [$\text{J}\cdot\text{m}^{-3}$]

$$E_V = \frac{P}{\Phi_V} = \frac{\Delta p \Phi_V}{\Phi_V} = \Delta p \tag{8}$$

in which P is the power input [W], and Φ_V is the volume flow [$\text{m}^3\cdot\text{s}^{-1}$]. For more than one pass the specific energy densities of all the passes are cumulative. This is further described in the results section.

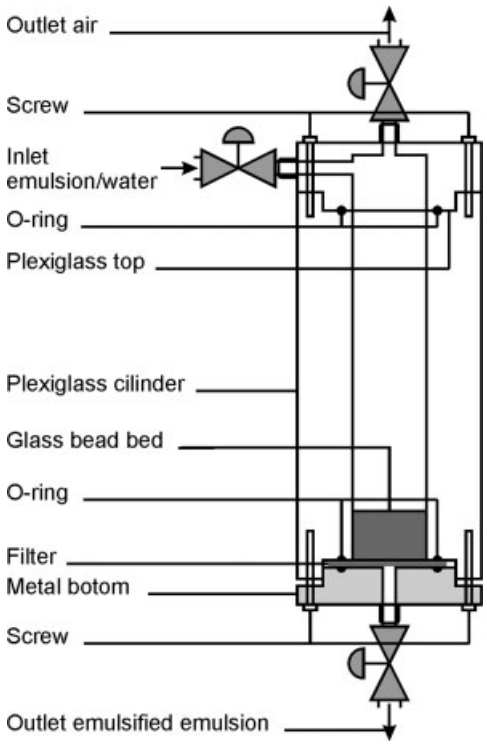

Figure 1. Column with glass beads.

Material and methods

n-Hexadecane (99% for synthesis, MERCK) was used as dispersed phase. MilliQ water (η_w = [0.001 Pa·s], ρ_w = [1,000 kg·m^{-3}]) was used as continuous phase. As surfactant Tween 20 (for synthesis, MERCK) was used. The concentration was in all cases 0.5% v/w water phase. The hexadecane fraction was in all cases 5% (v/v). The premix was made by stirring the continuous phase, the surfactant, and the dispersed phase with a magnetic stirrer at ~60 rpm in a 10 L flask for at least one day, because we found that after this time the premix droplet size leveled out. The total volume of the premix emulsion varied between 3 and 8 L, and in that way, a reproducible premix emulsion could be obtained.

For the particle bed, a fraction of 100HFL hydrophilic glass beads (Pneumix SMG-AF) obtained by sieving between a 53 μm and a 125 μm sieve were used. The average particle diameter ($d_{4,3}$) was measured to be 75.9 μm, and the span was 0.677. The particle density (ρ_p), and bulk density (ρ_b), were measured after sedimentation in water and found to be 2,518 kg·m^{-3} and 1,393 kg·m^{-3}, respectively, resulting in a particle holdup (ε) of 0.553 using

$$\varepsilon = \frac{\rho_b}{\rho_p} \tag{9}$$

Before the actual experiment started, a certain amount of glass beads (varying from 0 to 8 g) was put in the column as depicted in Figure 1. The filter on the bottom of the reactor that prevents the glass beads from falling out was a metallic Stork Veco sieve with rectangular pores of 10 by 405 μm, and a porosity of 4%. The column wall was made of Plexiglas to allow visual checking of the top surface of the glass bead bed, which is to be horizontal. The column was closed and connected to the rest of the setup (Figure 2).

At the beginning of the emulsification experiments, the valves connected to the pressurized nitrogen vessel, the water pressure vessel, and the outlet valve of the column with the particle bed were closed. The other valves were opened. Around 300 mL of the premix was put in the emulsion pressure vessel and by raising this vessel; the hydrostatic pressure difference transported the liquid to the column. Excess air in the reactor could escape through the air outlet. As soon as the column was filled with emulsion all valves going in and out of the reactor were closed. The column was turned up side down 3–5 times to disperse the glass beads through the liquid. The column was then placed vertically to let the particles settle to the bottom in a few seconds time. This pretreatment of the glass bead column lead to reproducible emulsification results, also slightly to our surprise.

The actual experiment was started by pressurizing the emulsion vessel. All valves connecting the nitrogen vessel with the column were opened. The pressure was set with the valve connected to the nitrogen, and read with the electronic pressure sensor (P). The outlet valve was opened and emulsification started; the homogenized emulsion was collected in a beaker on a balance connected to a computer, which recorded the mass output every second. The homogenized emulsion was recirculated up to six times. The droplet sizes of the premix emulsions, and the homogenized emulsions were analyzed with the Mastersizer 2000 of Malvern. After the entire experiment, the particles were cleaned repeatedly (3–4 times) with hot water.

The obtained curves (mass flow Φ_m [kg·s^{-1}] vs. time) were analyzed, and only if a linear relationship was obtained the data were used for further analysis. For example, creaming occurred in experiment with a relatively long duration, the curves are no longer linear because the actual viscosity was not constant in time, and, therefore, these data were disregarded. In total, 167 experiments qualified for the final analysis. The number of experiments per particle bed mass (m_{bed}), and number of passes (N) are shown in Table 1, together with the symbols that are used in the figures in the results and discussion section to distinguish them.

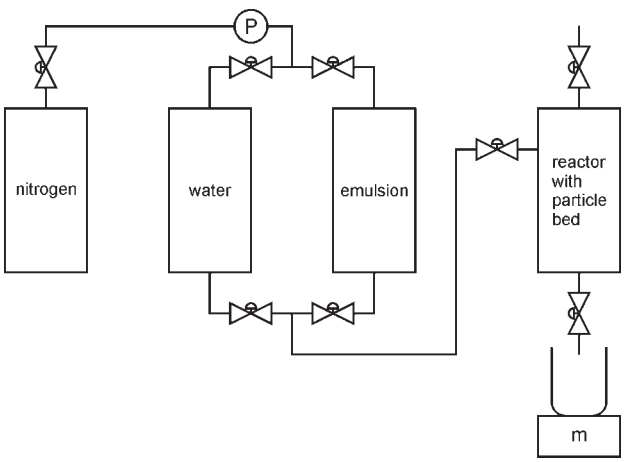

Figure 2. Experimental setup.

Table 1. Number of Experiments and Symbol Used in the Results and Discussion Section Particle Bed Mass (m_{bed}) and Number of Passes (N)

	N					
m_{bed}	1st	2nd	3rd	4th	5th	6th
filter	▼ 9	▼ 8	▼ 8	▽ 8	▽ 7	▽ 8
1 gram	■ 2	■ 4				
2 gram	◆ 9	◆ 10	◆ 8	◇ 10	◇ 6	◇ 8
4 gram	▲ 9	▲ 9	△ 10	△ 10	△ 9	△ 8
8 gram	★ 3	★ 4				

Gray scale indicates number of passes. Symbol shape indicated the bed height.

The droplet size was fitted for various pressures, mass flows, number of passes, and energy densities as described in the theory and results section. All fits were conducted with the MATLAB least-square fit function (lsqcurvefit) of the Optimization Toolbox and with the Mathcad minerr function. When both fits gave the same answer, the standard deviation of the fit, the standard deviation of the fit parameters, and the correlation coefficient for the parameters were calculated.

Results and Discussion

Effects of support sieve

To distinguish between the effect of the support sieve and the actual column, first the sieve was investigated separately with a 5 w/wt % emulsion of hexadecane in water. The pressure drop across the filter is plotted against the flux in Figure 3. We can see in the graph that there is no significant influence of the number of passes on the pressure drop. The line was fitted based on Eq. 5. The found values and standard deviations for the fit parameters are $\alpha_{filter} = (8.1 \pm 1.4)\ 10^6\ kg \cdot m^{-3}$ and $\beta_{filter} = (6.0 \pm 2.2)\ 10^5\ kg \cdot m^{-2} \cdot s^{-1}$. Given the range of conditions tested, these standard deviations are acceptable.

Characterization of the bed with Ergun equation

After the characterization of the support sieve, single pass experiments were carried out with beds of different mass. We will use mass (and not height), because the porosity of the bed, and, therefore, the height is not absolutely sure, while the mass is. In Figure 4, the pressure drop is plotted vs. the flux through the bed. The pressure increases nonlinearly with the flux as was expected from the Ergun equation (Eq. 1, indicated by the solid line), which implies a quadratic increase. As input parameters, the values from the list of symbols section were used. For the dynamic viscosity (η_l), and liquid density, the values for water were used (η_w and ρ_w). For the particle holdup (ε), the measured value as described in the results and material and methods section was used. The Ergun equation describes the data points for beds of 2 and 8 g very well, however, for beds of 1 and 4 g, the model either systematically under- or overestimates the data points.

Influence of particle bed porosity

The difference between the Ergun equation and the actual data points is probably a difference in particle holdup (ε) between experiments, caused by differences during the settling phase of the bed prior to the experiment. This effect was estimated by fitting the Ergun equation to the data points, but now allowing a variation in particles holdup (ε) for each mass of particles used (i.e., not for each separate experiment). The calculated values for the particle holdup and the bed height are listed in Table 2. The actual values that were calculated for the particle holdup are in a realistic range using the viscosity of water.

Important is that the results are not dependent on the number of passes. This indicates that although the droplet size and the number of droplets change with the number of passes, the viscosity, and, therefore, the permeation behavior is not affected too much.

Comparison with premix membrane emulsification

To determine whether our emulsification method is comparable to conventional premix membrane emulsification we plotted d_{50} [μm] values from Vladisavljević and coworkers,[6] and from our glass-bead experiments against the Energy density E_V [bar] calculated with Eq. 8 in Figure 5. We have chosen the Vladisavljević study, because it has the closest resemblance to our experiments. The values of the membrane experiments coincide well with the glass-bead bed experiments even though the dispersed phase (corn oil and hexadecane), and the dispersed phase concentration (40 w/v% and 5% v/v%) are different. The only exception is the result of the first pass, but this is most probably caused by the larger droplet size of the premix used for the membrane emulsification experiments. The comparability of these experiments leads us to believe that we can indeed use emulsification with a glass-bead bed as a model for premix membrane emulsification.

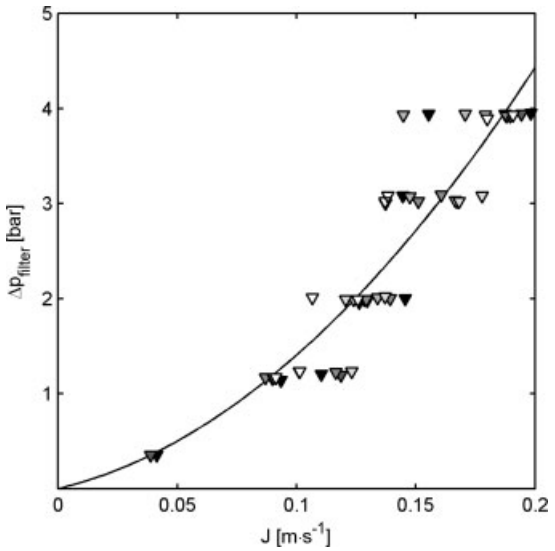

Figure 3. Pressure drop across the filter (Δp_{filter}) plotted against the flux (J).

The points are the measured data. The gray scale indicates the number of passes: black = 1 pass, white = 6 passes. The line is fitted with Eq. 5.

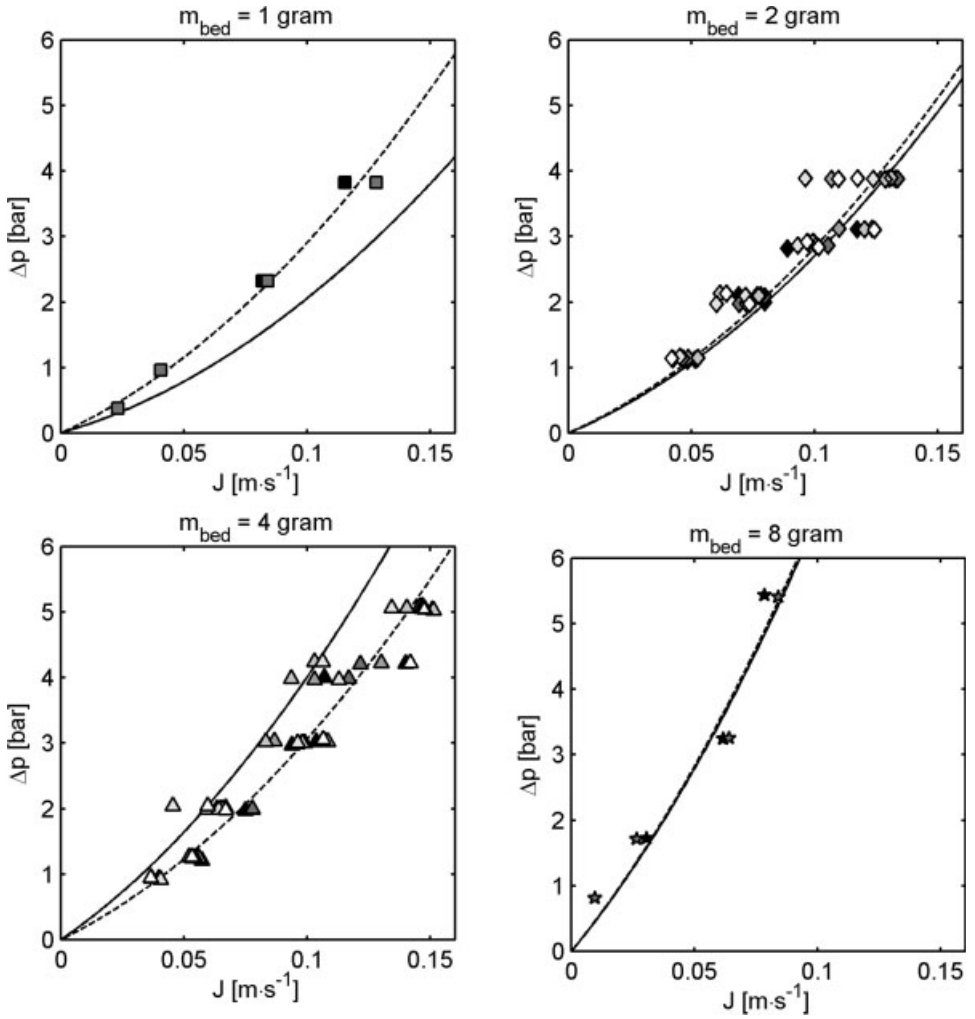

Figure 4. Pressure drop across the particle bed, and the filter (Δp) plotted against the flux (*J*) for four masses of particles (m_p) of the glass bead bed.

The points are the measured data. The gray scale of the points indicates the number of passes: black = 1 pass, and white = 6 passes. The solid line is calculated from theoretic data, and the dotted line is fitted. The fit values for the particle holdup are shown in Table 2.

Energy density approach for individual experiments

The Sauter mean droplet diameter $d_{3,2}$ (made dimensionless by division by [μm]) after homogenization was fitted to the specific energy density E_V (Eq. 7) for every bed height and each pass. The pressure drop Δp across the bed, and the filter was used for the calculation of the specific energy density. E_V was calculated cumulatively over all passes, and was made dimensionless by division by [bar]. The result is illustrated in Figure 6, in which four examples of measured Sauter mean diameters are shown as a function of the specific energy density together with the obtained fit for Eq. 7. In all cases, good descriptions of the experimental data were obtained; as expected, the droplet size decreased with increasing specific energy density and number of passes. The bed height H_{bed} however, does not increase the effectiveness of the homogenization. More energy is needed to reach the same droplet size for a particle bed compared to the filter-only experiments. The particle bed does, however, decrease the span of the resulting droplets as shown in Table 3. The effectiveness of emulsification is related to the parameters in Eq. 7, which are investigated in the following paragraphs.

Table 2. Fit Values for the Particle Holdup (ε) and Bed Height (H_{bed})

m_{bed}	ε	H_{bed}	H_{bed} / d_p
filter			1
1 gram	0.625	1.9 mm	25.5
2 gram	0.561	4.3 mm	56.7
4 gram	0.510	9.5 mm	125
8 gram	0.554	17.4 mm	230

In Figure 7 parameters α_{drop} and β_{drop}, from Eq. 7, are plotted as a function of bed height divided by the diameter of the particles (H_{bed}/d_p), and the number of passes (N). The term H_{bed}/d_p is an indication for the number of particle layers. For the experiments with only the filter this term was set at unity (see Table 2 for values of this term). Also the standard deviations of the fit parameters are shown in the figure as error bars. The parameters α_{drop} and β_{drop} do not change significantly as a function of the bed height (the two

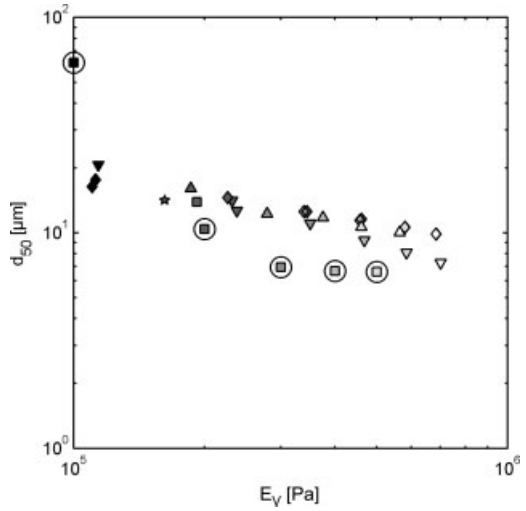

Figure 5. Average droplet diameter (d_{50}) as a function of energy density (E_V) for emulsion homogenization with a membrane, and with a particle bed.

The circled squares are the membrane values taken from Figure 11 of Vladisavljević et al.[6] (Tween 20 concentration = 0.5 wt%, $\Delta p_{membrane} = 10^5$ Pa). All other symbols are comparable particle bed values (Tween 20 concentration = 0.5 wt%, $0.8 \cdot 10^5$ Pa $< \Delta p < 1.2 \cdot 10^5$ Pa). The gray scale of the points indicates the number of passes: black = 1 pass, white = 6 passes. See Table 1 for an explanation of the symbols.

graphs on the lefthand side), even though we expected an influence of the bed height, and, thus, the number of layers. The reason may be that the actual number of layers of particles used in the beds always exceeds the optimum number of layers lays by far; the optimum is around four layers according to Van der Zwan and coworkers.

As a function of the number of passes the α_{drop} parameter increases. If only the filter is used for experimentation, a plateau value is reached after three passes. For experiments carried out with glass beads a plateau is also found, albeit at a higher pass number (see top right graph in Figure 7). The increase in the value of α_{drop} indicates a decrease in effectiveness of the homogenization. Not all energy inserted in the system is used to breakup the droplets, and more energy is lost due to coalescence with progressive number of passes. Besides that we see the β_{drop} parameter increases with increasing number of passes, therefore, indicating that the flow regime is changing. This latter effect can counteract the energy losses due to coalescence described previously, due to turbulence.

Table 3. Span Values for a Selection of the Measured Droplet Size Distributions at a Pressure Drop of Around 2 Bar

m_{bed}	Span
filter	1.689
1	1.498
2	1.294
4	1.254
8	1.321

Extended overall energy density approach

To check the general validity of the energy density approach we fitted all data to Eq. 7, and two extended versions thereof (Eqs. 10 and 11)

$$d_{3,2} = \alpha_{drop} E_V^{-\beta_{drop}} N^{\gamma_{drop}} \tag{10}$$

$$d_{3,2} = \alpha_{drop} E_V^{-\beta_{drop}} N^{\gamma_{drop}} \left(\frac{H_{bed}}{d_p}\right)^{\delta_{drop}} \tag{11}$$

in which $d_{3,2}$ is the Sauter diameter of the droplets after N passes, E_V is the total specific energy density after N passes, H_{bed} is the height of the bed, d_p is the particle size of the

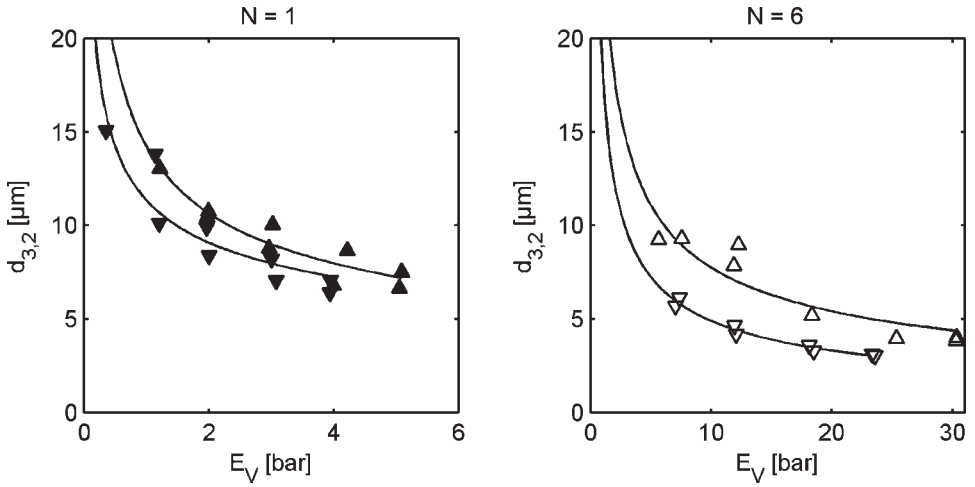

Figure 6. Four examples of the Sauter diameter after homogenization ($d_{3,2}$) plotted against the specific energy density (E_V), or pressure drop (Δp) with the line fitted with Eq. 7.

Downward pointing triangles indicate that the experiments were conducted with the filter only. Upward pointing triangles indicate that the experiments were conducted with a bed height H_{bed} of 9.5 mm.

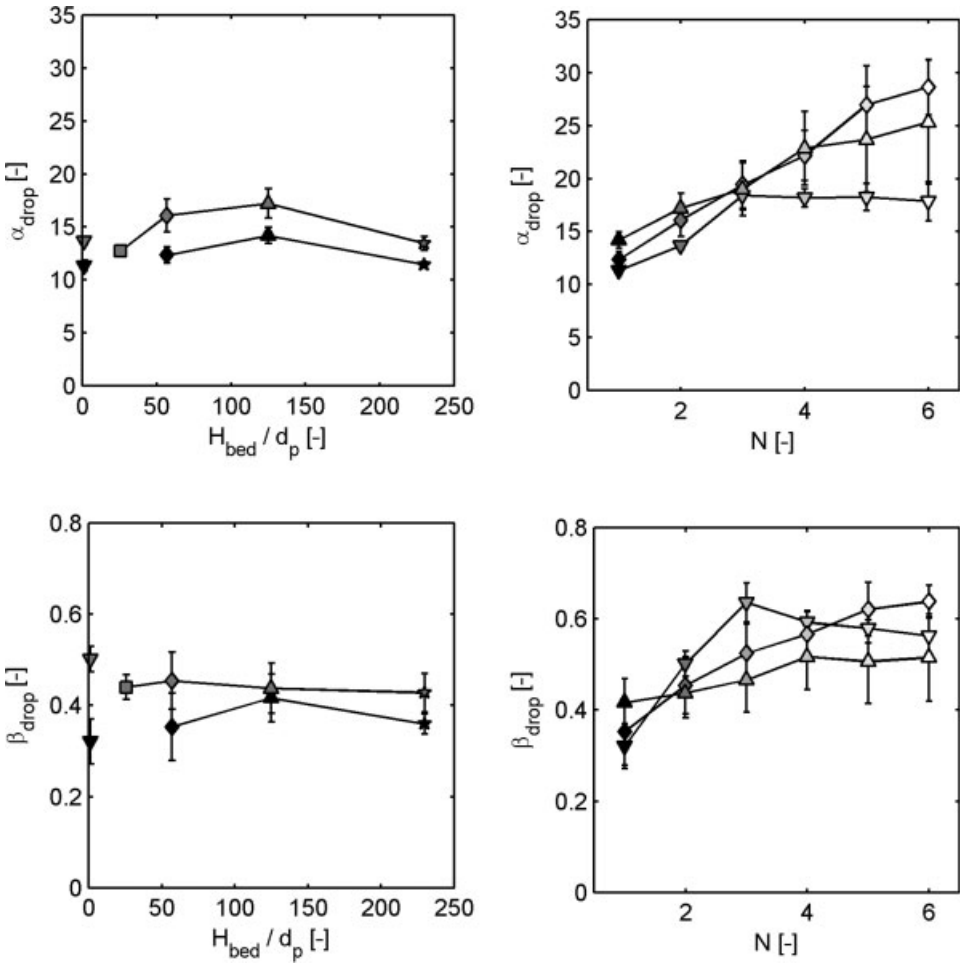

Figure 7. Parameters α_{drop} (top) β_{drop} (bottom) plotted against the bed height H_{bed} (left, for $N = 1$ and $N = 2$), and the number of passes N (right, for the filter only, and for particle bed mass $m_{bed} = 2$ g, and $m_{bed} = 4$ g).

See Table 1 for an explanation of the symbols. The error bars indicate the standard deviation of parameters α_{drop} and β_{drop}.

glass beads in the bed, and α_{drop}, β_{drop}, γ_{drop}, and δ_{drop} are fit parameters. Equation 10 is the energy approach extended with the influence of the number of passes, which was clearly visible in Figure 7. Equation 11 is the energy density approach extended for the influence of both the number of passes and the bed height.

In Table 4, the calculated values of the fit parameters are shown together with their standard deviations. In the sixth row of Table 4 the standard deviation in the prediction of the model ($\sigma_{model}[\mu m]$) is given. The bottom row of Table 4 gives the Akaike criterion (*AIC*) for every model defined as

$$AIC = n \ln\left(\frac{SS}{n}\right) + 2(p+1) \tag{12}$$

in which n is the number of data point, p is the number of parameters, and *SS* is the residual sum of the squares. The Akaike criterion indicates the probability of the model; the model with the lowest *AIC* is most probable. In Figure 8, the measured Sauter diameter is plotted against the result of Eqs. 7, 10 and 11, respectively, with the fit parameters from Table 4.

From the figure and table it is clear that Eq. 11 predicts $d_{3,2}$, the best of all models. Even though the model requires more parameters it has the lowest *AIC*, and this indicates that the use of extra parameters is justified, and improves the fit. The correlation coefficients between the four fit parameters are shown in Table 5; they all have such values that it is clear that they are all not correlated. Furthermore, the parameters show high-reliability (or low-standard deviation); therefore, we expect that the proposed equation is a robust tool to describe premix (membrane) emulsification.

Table 4. Values and Standard Deviations of the Fit Parameters and Akaike Criterion for Eqs. 7, 10 and 11

	Equation 7	Equation 10	Equation 11
α_{drop}	13.3 ± 0.436	14.0 ± 0.441	12.1 ± 0.304
β_{drop}	0.366 ± 0.0187	0.483 ± 0.0296	0.557 ± 0.0205
γ_{drop}		0.179 ± 0.0366	0.275 ± 0.0255
δ_{drop}			0.0625 ± 0.00490
σ_{model}	1.254 μm	1.166 μm	0.783 μm
AIC	70.89	50.31	−66.56

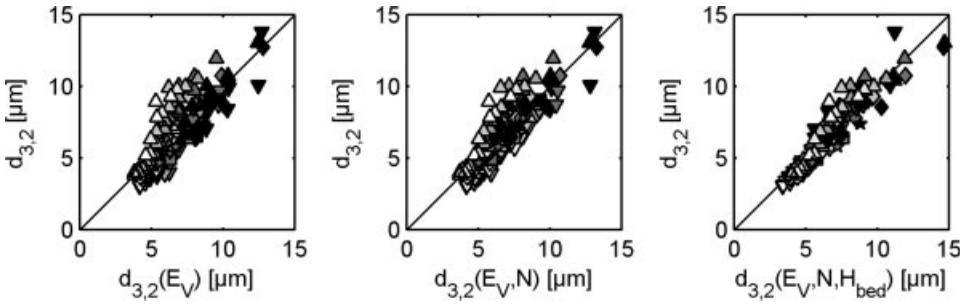

Figure 8. Measured values of the Sauter diameter $d_{3,2}$ plotted against the result of Eq. 7 or $d_{3,2}(E_v)$, Eq. 10 or $d_{3,2}(E_v,N)$, and Eq. 11 or $d_{3,2}(E_v,N,H_{bed})$, with the fit parameters from Table 4.

See Table 1 for an explanation of the symbols.

Table 5. Correlation Coefficients Between the Fit Parameters of Eq. 11

	α_{drop}	β_{drop}	γ_{drop}	δ_{drop}
α_{drop}		0.45	0.08	0.55
β_{drop}	0.45		0.83	0.25
γ_{drop}	0.08	0.83		0.26
δ_{drop}	0.55	0.25	0.26	

Conclusion

Using a packed layer of small particles may well be a robust alternative for premix membrane emulsification, where the formulation would cause internal fouling of the membrane pores. Droplet sizes produced with the packed bed could be described accurately for various bed heights, number of passes, and pressures by using an extended energy density approach. The parameters could be determined with high-statistic relevance; therefore, it is expected that the equation can be used to design a processes for a required droplet size.

Notation

Latin symbols

A_{col} = column surface area, m^2
AIC = Akaike criterion
d_p = glass bead particle diameter, μm
E_V = specific energy density, $J \cdot m^{-3}$
H_{bed} = particle bed height, m
J = flux across the bed, $m^3 \cdot s^{-1} \cdot m^{-2} = m \cdot s^{-1}$
m_{bed} = particle bed mass, gram
N = number of passes through the particle bed
n = number of data points
P = power input, W
p = number of parameters
SS = residual sum of squares
v_{sl} = superficial liquid speed, $m \cdot s^{-1}$

Greek letters

Δp = pressure drop across the bed and the filter, Pa
Δp_{bed} = pressure drop across the bed, Pa
Δp_{filter} = pressure drop across the filter, Pa
$\Delta p_{membrane}$ = pressure drop across the membrane, Pa
ε = particle holdup
η_l = dynamic liquid viscosity, $Pa \cdot s$
η_w = dynamic liquid viscosity of water, $Pa \cdot s$
ρ_b = specific bulk density $kg \cdot m^{-3}$
ρ_l = specific liquid density, $kg \cdot m^{-3}$
ρ_w = specific liquid density of water $kg \cdot m^{-3}$
ρ_p = specific particles density, $kg \cdot m^{-3}$
σ_{model} = standard deviation of the prediction of the model, μm
Φ_m = mass flow, $kg \cdot s^{-1}$
Φ_V = volume flow, $m^3 \cdot s^{-1}$

Fit parameters

α_{filter}, β_{filter} = fit parameters for the pressure drop Eq. 5, $kg \cdot m^{-3}$, $kg \cdot m^{-2} \cdot s^{-1}$
α_{drop}, β_{drop} = fit parameters for the energy density approach
γ_{drop}, δ_{drop} = Eqs. 7, 10 and 11

Literature Cited

1. Suzuki K, Fujiki I, Hagura Y. Preparation of corn oil/water and water/corn oil emulsions using PTFE membranes. *Food Sci Technol Int Tokyo*. 1998;4(2):164.
2. Altenbach-Rehm J, Suzuki K, Schubert H. In: Production of O/W-emulsions with narrow droplet size distribution by repeated premix membrane emulsification. Third World Congress on Emulsions (CME3); 2002/09/24; p 051; Lyon, France.
3. Lambricht U, Vladisavljevic GT. Emulsification using microstructured systems. *Chemie Ingenieur Technik*. 2004;76(4):376.
4. Suzuki K, Ohwan Y, Hagura Y. In: Properties of solid fat O/W emulsions prepered by membrane emulsification method combined with pre-emulsification. Third World Congress on Emulsions (CME3); 2002/09/24/; p 114; Lyon, France.
5. Vladisavljevic GT, Shimizu M, Nakashima T. Preparation of monodisperse multiple emulsions at high production rates by multi-stage premix membrane emulsification. *J Membr Sci*. 2004;244:97.
6. Vladisavljevic GT, Surh J, McClements JD. Effect of emulsifier type on droplet disruption in repeated Shirasu porous glass membrane homogenization. *Langmuir*. 2006;22(10):4526–4533.
7. Van der Zwan E, Schroen K, Van Dijke K, Boom R. Visualization of droplet break-up in pre-mix membrane emulsification using microfluidic devices. *Coll Surf a-Physicochem Eng Aspects.* 2006; 277(1–3):223–229.
8. Van 't Riet K. *Basic Bioreactor Design*. 1st ed. Marcel Dekker, Inc: New York; 1991.
9. Karbstein H, Schubert H. Developments in the continuous mechanical production of oil-in-water macro-emulsions. *Chem Eng Proc*. 1995;34(3):205–211.
10. Schröder V. Herstellen von Öl-in-Wasser-Emulsionen mit mikroporösen Membranen. Universität Karlsruhe (TH); 1999. PhD.

Manuscript received Jun. 25, 2007, and revision received Mar. 16, 2008.